Elastic backscattering measurements for ^{6}Li + ^{28}Si at sub- and near-barrier energies

K. Zerva,[1] N. Patronis,[1] A. Pakou,[1,*] N. Alamanos,[2] X. Aslanoglou,[1] D. Filipescu,[3] T. Glodariu,[3] M. Kokkoris,[4] M. La Commara,[5] A. Lagoyannis,[6] M. Mazzocco,[7] N. G. Nicolis,[1] D. Pierroutsakou,[8] M. Romoli,[8] and K. Rusek[9]

[1]*Department of Physics, The University of Ioannina, GR-45110 Ioannina, Greece*
[2]*DSM/DAPNIA CEA SACLAY, F-91191 Gif-sur-Yvette, France*
[3]*"Horia Hulubei" National Institute of Physics and Nuclear Engineering, Bucharest-Magurele, Romania*
[4]*National Technical University of Athens, Athens, Greece*
[5]*Dipartimento di Scienze Fisiche and INFN Sezione di Napoli, I-80125, Napoli, Italy*
[6]*National Research Center Demokritos, Agia Paraskevi, Greece*
[7]*Dipartimento di Fisica, INFN, I-35131 Padova, Italy*
[8]*INFN Sezione di Napoli, I-80125, Napoli, Italy*
[9]*Heavy Ion Laboratory, University of Warsaw, Pasteura 5a, PL-02-093 Warsaw, Poland*

(Received 27 May 2009; published 31 July 2009)

Elastic backscattering measurements were performed for the weakly bound nucleus ^{6}Li on a ^{28}Si target at sub- and near-barrier energies (0.6 to 1.3 $V_{C.B.}$). Excitation functions of elastic scattering cross sections were measured at 150° and 170° and the corresponding ratios to Rutherford scattering and relevant barrier distributions were formed. The results are discussed in terms of the potential threshold anomaly and the reaction mechanisms involved.

DOI: 10.1103/PhysRevC.80.017601 PACS number(s): 25.70.Bc, 24.10.Ht, 24.50.+g

As is well known for heavy ion reactions, approaching the vicinity of the Coulomb barrier, couplings between various channels increase in importance. Describing elastic scattering, either these couplings have to be taken into account through coupled channel theories, or the energy dependence of the various optical model parameters has to be considered explicitly. In fact, the term "threshold anomaly" was invoked to describe a rapid variation of such model parameters around the barrier in well bound nuclei. In that respect, near- and sub-barrier fusion cross sections have been reproduced [1,2] by using a single barrier penetration model with an energy dependent potential corresponding to the threshold anomaly. Moving to weakly bound nuclei the situation becomes more complicated due to the influence of breakup and/or transfer effects. In fact for ^{6}Li, in contrast to the well bound nuclei, an absence of the threshold anomaly was reported previously [3,4], while later, an increasing trend approaching the barrier from above was established for the imaginary part of the optical potential [5,6]. This was related to a rather flat or slightly curved with negative slope trend for its real part, in accordance with dispersive relations. The proposed new type of anomaly was based on a systematic data analysis of ^{6}Li elastic scattering on various targets (^{28}Si, ^{58}Ni, ^{118}Sn, ^{208}Pb) measured previously [3,5,7], in the context of the double folding model [8] by using the BDM3Y1 interaction developed by Khoa *et al.* [9]. This trend, verified in [10,11] by using the Sao Paulo potential [12], was attributed to breakup and therefore named as a breakup anomaly. In principle, the intrinsic lack of sensitivity for obtaining the energy dependence of potential parameters, at energies close to the Coulomb barrier, leads occasionally to vague conclusions, while the determination of such dependence at sub-barrier energies is almost impossible. In order to improve our understanding on the energy dependence of the potential especially at sub-barrier energies and the relevant processes involved in the threshold anomaly, other complementary means should be adopted. In this respect, we test in this work excitation functions of backscattering measurements as a tool for probing the new type potential anomaly for weakly bound nuclei, and for extending the energy dependence of the optical potential at sub-barrier energies. The last years a large amount of work has been devoted on systematic studies of the nuclear potential surface properties through high precision back-angle quasi-elastic scattering measurements [13–18] at sub-barrier energies. At these backward angle studies, deviations from unity of the elastic to Rutherford cross section ratios, are sensitive mainly to the surface properties of the potential [14]. Moreover, barrier distributions of elastic [19] and quasi-elastic scattering [20], obtained via first derivatives as follows:

$$D_{\mathrm{el}}(E) = -\frac{d}{dE}\left[\sqrt{\frac{d\sigma_{\mathrm{el}}}{d\sigma_{\mathrm{Ruth}}}(E)}\right], \qquad D_{\mathrm{qel}}(E) = -\frac{d}{dE}\left[\frac{d\sigma_{\mathrm{qel}}}{d\sigma_{\mathrm{Ruth}}}(E)\right] \tag{1}$$

have been used mainly on research with stable projectiles to probe channel coupling effects at barrier energies [19–25], in almost the same effective way as barrier distribution from fusion measurements, initially presented in Ref. [26].

The influence of direct processes on elastic scattering and other reaction channels with weakly bound nuclei has been reviewed in [27,28]. A first measurement with a weakly bound projectile has been performed recently on ^{6}Li+^{144}Sm and reports backward elastic and quasi-elastic barrier distributions [29] with emphasis on breakup coupling to elastic scattering. For the system ^{6}Li+^{28}Si, strong transfer channels were reported in [30–32] while a weak breakup channel was

*Corresponding author: apakou@cc.uoi.gr

reported in [33]. Then, the arising question is: Does transfer or breakup influence elastic scattering and the other reaction processes at barrier energies? In the following, we report a back-angle elastic scattering excitation function measurement for ^{6}Li+^{28}Si at sub- and near-barrier energies aiming to further enlighten the subjects stated above, concerning the new type of potential anomaly and relevant reaction mechanisms. Experimental data were analyzed with an energy dependent optical potential satisfying the dispersion relation, taking care for a reproduction of previously measured total reaction and fusion cross sections [32]. The results were considered also in the context of a coupled channel description, where breakup is explicitly taken into account. ^{6}Li^{3+} beams were delivered by the TN11/25 HVEC 5.5 MV Tandem accelerator of the National Research Center of Greece-DEMOKRITOS at several bombarding energies, from 5 to 11 MeV. Beam currents were of the order of 5 nA. The beam impinged on a 200 μg/cm^2 thick, self-supporting ^{28}Si target, at a target frame fixed perpendicular to the beam direction. Backscattering elastic events were recorded in four silicon detectors set at $\pm$150 and $\pm$170 degrees. The beam flux was recorded via the Rutherford scattering in two silicon detectors set at $\pm$30 degrees. Subsequently elastic cross section ratios to Rutherford were formed as follows:

$$\frac{\sigma_{\rm el}}{\sigma_{\rm Ruth}}(170^\circ - 150^\circ) = \frac{N(170^\circ - 150^\circ)}{N(30^\circ)} \frac{\sigma_{\rm Ruth}(30)}{\sigma_{\rm Ruth}(170)} \frac{\Omega_{30}}{\Omega_{170(150)}}, \qquad (2)$$

where N_{30} and $N_{170(150)}$ are the elastic scattering total counts at forward and backward detectors, and $\Omega_{30}, \Omega_{170(150)}$ are the solid angles subtended by the forward and backward detectors. The ratio of solid angles was determined in the same experiment by using a thin gold target and by using lithium ions at 11 MeV. At this energy, the elastic scattering is pure Rutherford for both forward and backward detectors, and the ratio of solid angles can be determined with a negligible error. Therefore the only error involved in relation (2) is the statistical error which in most of the energies was less than 2%, except at the highest energies which was up to 20%. The obtained excitation functions are presented in Fig. 1(a) and the corresponding barrier distributions, determined by using a point difference formula for extracting the derivative of relation (2)-first expression, are presented in Fig. 1(b). It should be noted that the results presented in Fig. 1 are error-weighted means of the cross sections obtained at 150 and 170 degrees. This was done to increase the statistics and it was possible, since the energy centrifugal correction was negligible ($\sim$1.0%) for these angles. A first inspection of this figure shows the absence of the usual second peak at energies above the nominal coulomb barrier related to inelastic excitations. This was expected however, since preliminary coupled channel calculations with the code ECIS showed that inelastic excitations of target are negligible and such couplings can be omitted. Also in our particle spectra peaks due to inelastic excitation of target were not present to an extend of cross section production less than 2 mb at the highest energy.

Having obtained experimentally excitation functions and barrier distributions, we proceed with our theoretical analysis.

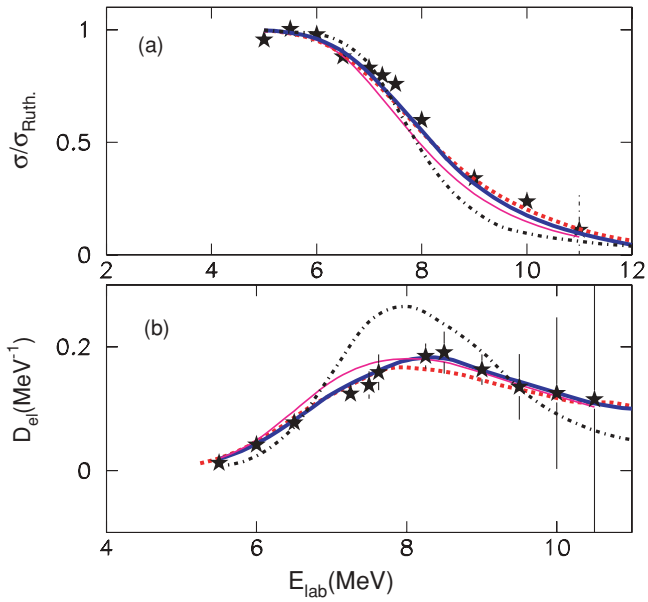

FIG. 1. (Color online) (a) Elastic cross sections (designated by stars), an error-weighted mean of measured cross sections at 150° and 170°, as a function of energy for ^{6}Li+^{28}Si. The lines represent ECIS calculations with the optical potential presented in Fig. 2, with the same notation. The dotted-dashed line (black line) corresponds to a decreasing imaginary potential from higher to lower energies, the solid line (blue line) corresponds to an increasing imaginary potential which best fits the backscattering data, the thin solid line (pink line) the same imaginary potential but which drops to zero earlier and finally the dashed line (red line) represents a potential with an increasing trend from above but with steepest slope. (b) Elastic backscattering barrier distributions, with the same notation as in (a).

In Fig. 2 we present previous data on the potential anomaly, obtained in a folding framework [5] with a BDM3Y1 interaction. While the increasing trend was obvious for the heavier targets as is seen in [5], for ^{28}Si due to the large assigned errors this is not clear. In the following analysis, in order to describe the imaginary part of the potential, we start with a line with decreasing slope from higher to lower energies as appears in the conventional anomaly of well bound nuclei. The corresponding real part is calculated via dispersive relations [34]. With this optical potential, elastic scattering cross sections are calculated for backward angles (150° and 170°). The results, a mean of cross sections at 150° and 170°, are presented in Fig. 1(a). The corresponding barrier distributions are presented in Fig. 1(b). It is obvious, that such a trend for the imaginary potential is totally excluded for the system ^{6}Li+^{28}Si. Subsequently we have varied the slope of the line, changing it from negative to positive values and each time repeating the above procedure. The results, obtained with the potential, shown in Fig. 2 with the solid line (blue line), represent the experimental barrier distribution in a satisfactory way and it is adopted as the "best" optical potential. To show further the sensitivity of this test on the magnitude of a positive slope we draw also a line with a steeper slope, designated in Fig. 2 with a dashed line (red line). The steepest slope corresponds to a flat barrier distribution shifted to the left off our experimental barrier distribution. As the slope is reduced

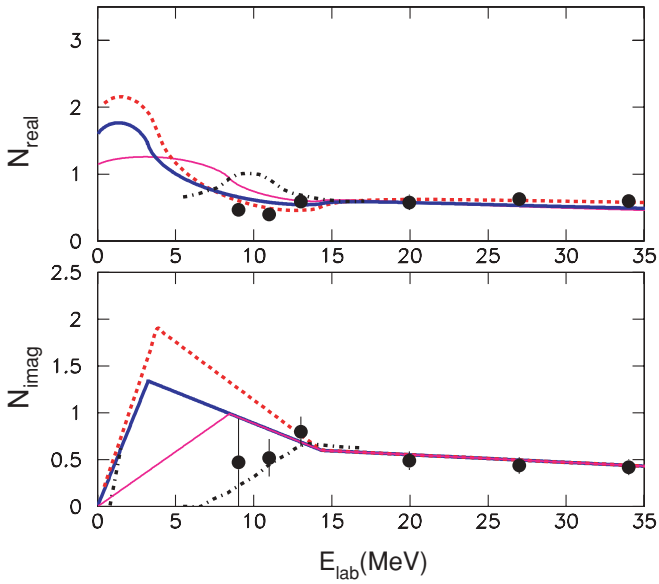

FIG. 2. (Color online) Previously determined normalization factors of the real and imaginary potential as a function of the lithium bombarding energy [5,6], designated with solid circles. For the imaginary potential we have assumed three different descriptions (dotted-dashed black, dashed red, solid blue, and thin solid pink lines). The corresponding real potential was calculated via dispersive relations [34].

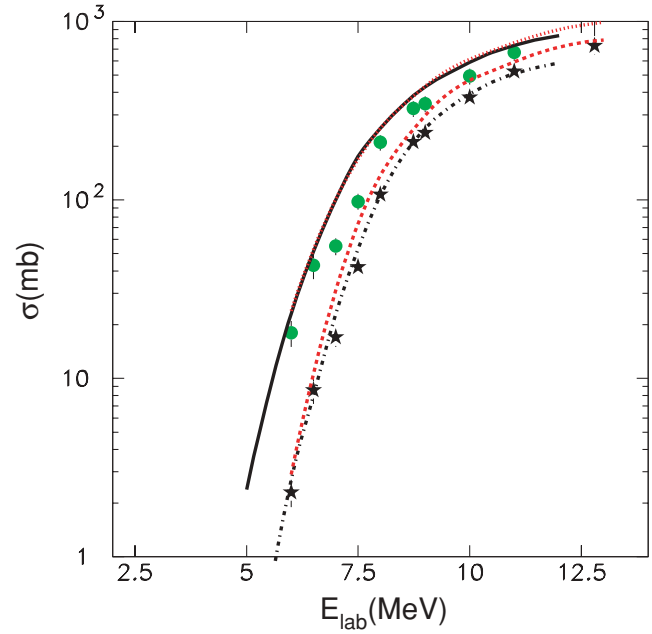

FIG. 3. (Color online) Total reaction (green circles) and fusion cross section (black stars) measurements as a function of energy reported previously [32]. The black solid and dotted-dashed lines are ECIS calculations for total reaction and fusion cross sections respectively, corresponding to the "best" optical potential (Fig. 2, blue line). The red dotted and dashed lines show coupled channel calculations for the total reaction and fusion cross sections, respectively.

the barrier distribution is shifted to the right and the height of the barrier distribution increases. The connection between the slope of the line describing the imaginary potential and the involved direct process (breakup or/and transfer) and the used target, is not straight forward and needs further investigation. In that direction complementary measurements with lighter and heavier targets are under the way. Last, in order to attempt an extend of the energy dependence of the optical potential to lower energies, we have to fix additionally the point after which the potential drops to zero. From Fig. 2 we see that, if we choose an "early" drop of the potential, designated with a thin solid line (pink line), the barrier distribution while keeps the height of its maximum has been moved to the left. It has become clear with the above analysis that barrier distributions of elastic scattering can be proved a valuable tool for tracing the threshold anomaly. Moreover, it can be used to further extend below barrier the energy dependence of the optical potential. To complete our analysis, we present in Fig. 3 previously measured [32] excitation functions of total reaction (green circles) and fusion cross sections (black stars). The experimental results are compared with calculations obtained with the above obtained "best" potential (black lines) and the code ECIS. The reproduction of the data is fair for the total reaction cross sections and very good for the fusion cross sections. Subsequently we proceed with calculations in a coupled channel approach taking into account breakup. Our calculations followed closely those presented in [6]. Two body, $\alpha + d$ cluster model of ^{6}Li was assumed. The continuum above the $^6\text{Li} \rightarrow \alpha + d$ breakup threshold was truncated at momentum $k = 0.52$ fm^{-1} and discretized into momentum bins of the 0.26 fm^{-1} width. Couplings between resonant and nonresonant cluster states corresponding to $\alpha - d$ relative orbital angular momentum $L = 0, 1, 2$ were taken into account by means of continuum-discretized coupled-channels method. Two resonances, at 2.18 MeV and

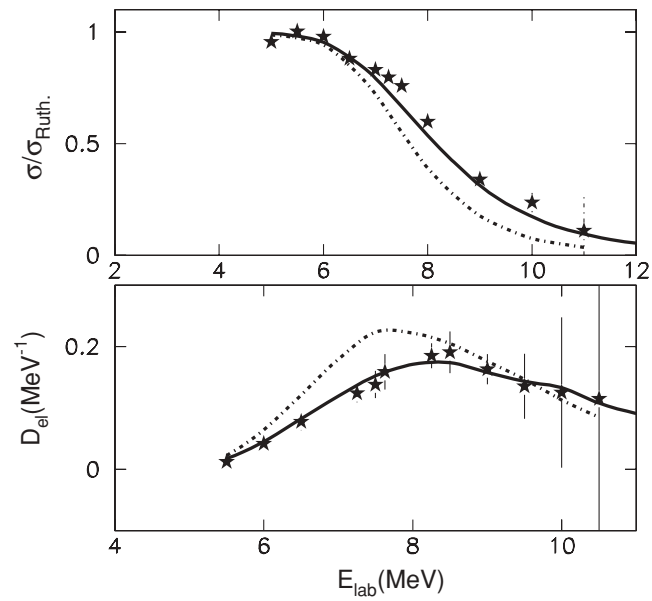

FIG. 4. The elastic scattering data and corresponding barrier distributions, presented in Fig. 1, are compared with coupled channel calculations (dotted dashed line: calculations with no coupling, solid line: coupled channel calculations).

4.31 MeV of excitation energy, were also included. The diagonal and coupling potentials were calculated from empirical $\alpha + {}^{28}$Si and $d + {}^{28}$Si optical model potentials by means of the single-folding technique. The results of the calculations are presented in Fig. 4 with the solid curves: Fig. 4(a) for the elastic scattering and Fig. 4(b) for the barrier distribution, and show very good agreement with the data. The dotted-dashed curves represent results of optical model calculations, without couplings to the breakup states from the continuum included. It is seen, that moving from calculations with no coupling to calculations with coupling to breakup, the distribution presents a broadening and a decrease of its barrier height, consistent with the known properties of the polarization potential for breakup. In Fig. 3, the results of calculations for the total reaction cross section and the fusion cross section are plotted and show fair agreement with the data. The fusion cross section was calculated by means of barrier penetration model with an energy dependent effective potential. This potential consisted of the diagonal "bare" potential used as an input to coupled channel calculations and the polarization potential. The latter was derived from coupled channel calculations using the "weighted trivial equivalent" method as described in [35]. In conclusion, we have shown that by determining experimentally barrier distributions via elastic scattering at backward angles we have an additional tool to map the optical potential at near- and sub-barrier energies, where weakly bound nuclei present the new type of threshold anomaly. The proposed method, is especially useful for extending the energy variation of the optical potential at sub-barrier energies, where the nuclear field is weak and manifested only at very backward-angle data. Our coupled channel analysis shows that breakup, although a weak channel for the studied system, is a strong channel coupling element at barrier energies. On the other hand, the influence of transfer, which is a strong direct channel at sub- and near-barrier energies, has to be also investigated.

[1] G. R. Satchler, Phys. Rep. **199**, 147 (1991).
[2] M. A. Nagarajan and G. R. Satchler, Phys. Lett. **B173**, 29 (1986).
[3] N. Keeley *et al.*, Nucl. Phys. **A571**, 326 (1994).
[4] A. M. M. Maciel *et al.*, Phys. Rev. C **59**, 2103 (1999).
[5] A. Pakou *et al.*, Phys. Lett. **B556**, 21 (2003).
[6] A. Pakou *et al.*, Phys. Rev. C **69**, 054602 (2004).
[7] K. O. Pfeifer, E. Speth, and K. Bethge, Nucl. Phys. **A206**, 545 (1973).
[8] G. R. Satchler and W. G. Love, Phys. Rep. **55**, 183 (1979).
[9] D. T. Khoa *et al.*, Phys. Lett. **B342**, 6 (1995).
[10] M. S. Hussein, P. R. S. Gomes, J. Lubian, and L. C. Chamon, Phys. Rev. C **76**, 019902(E) (2007).
[11] J. M. Figueira *et al.*, Phys. Rev. C **75**, 017602 (2007).
[12] M. A. Cândido Ribeiro, L. C. Chamon, D. Pereira, M. S. Hussein, and D. Galetti, Phys. Rev. Lett. **78**, 3270 (1997).
[13] I. I. Gontchar, D. J. Hinde, M. Dasgupta, and J. O. Newton, Nucl. Phys. **A722**, 479c (2003).
[14] K. Hagino, T. Takehi, A. B. Balantekin, and N. Takigawa, Phys. Rev. C **71**, 044612 (2005).
[15] K. Washiyama, K. Hagino, and M. Dasgupta, Phys. Rev. C **73**, 034607 (2006).
[16] L. R. Gasques *et al.*, Phys. Rev. C **76**, 024612 (2007).
[17] O. A. Capurro, N. J. O. Fernandez, A. J. Pacheco, and P. R. S. Gomes, Phys. Rev. C **75**, 047601 (2007).
[18] M. Evers *et al.*, Phys. Rev. C **78**, 034614 (2008).
[19] N. Rowley *et al.*, Phys. Lett. **B373**, 23 (1996).
[20] H. Timmers *et al.*, Nucl. Phys. **A584**, 190 (1995).
[21] H. Timmers *et al.*, J. Phys. G **23**, 1175 (1997).
[22] H. Timmers *et al.*, Nucl. Phys. **A633**, 421 (1998).
[23] R. F. Simoes *et al.*, Phys. Lett. **B527**, 187 (2002).
[24] E. Piasecki *et al.*, Phys. Rev. C **65**, 054611 (2002).
[25] J. M. B. Shorto *et al.*, Phys. Rev. C **78**, 064610 (2008).
[26] N. Rowley, G. R. Satchler, and P. H. Stelson, Phys. Lett. **B254**, 25 (1991).
[27] L. F. Canto, P. R. S. Gomes, R. Donangelo, and M. S. Hussein, Phys. Rep. **424**, 1 (2006).
[28] N. Keeley, R. Raabe, N. Alamanos, and J. L. Sida, Prog. Part. Nucl. Phys. **59**, 579 (2007).
[29] D. S. Monteiro *et al.*, Phys. Rev. C **79**, 014601 (2009).
[30] A. Pakou *et al.*, Phys. Rev. C **76**, 054601 (2007).
[31] A. Pakou, Phys. Rev. C **78**, 067601 (2008).
[32] A. Pakou *et al.*, Eur. Phys. J. A **39**, 187 (2009).
[33] A. Pakou *et al.*, Phys. Lett. **B633**, 691 (2006).
[34] M. A. Nagarajan, C. C. Mahaux, and G. R. Satchler, Phys. Rev. Lett. **54**, 1136 (1985).
[35] I. J. Thompson, M. A. Nagarajan, J. S. Lilley, and M. J. Smithson, Nucl. Phys. **A505**, 84 (1989).